Inorg. Chem. **2003**, *42*, 974–981

A Complete Family of Isostructural Cluster Compounds with Cubane-like M_3S_4M' Cores (M = Mo, W; M′ = Ni, Pd, Pt): Comparative Crystallography and Electrochemistry

Konrad Herbst,*,† Piero Zanello,‡ Maddalena Corsini,‡ Nicola D'Amelio,‡ Lutz Dahlenburg,§ and Michael Brorson†

Haldor Topsøe A/S, Nymøllevej 55, DK-2800 Lyngby, Denmark, Dipartimento di Chimica dell'Università di Siena, Via Aldo Moro, I-53100 Siena, Italy, and Institut für Anorganische Chemie, Universität Erlangen-Nürnberg, Egerlandstrasse 1, D-91058 Erlangen, Germany

Received September 5, 2002

By reaction of the geometrically incomplete cubane-like clusters $[(\eta^5\text{-Cp}')_3Mo_3S_4)][pts]$ and $[(\eta^5\text{-Cp}')_3W_3S_4][pts]$ (Cp′ = methylcyclopentadienyl; pts = *p*-toluenesulfonate) with group 10 alkene complexes, three new heterobimetallic clusters with cubane-like cluster cores were isolated: $[(\eta^5\text{-Cp}')_3W_3S_4M'(PPh_3)][pts]$ ([**5**][pts], M′ = Pd; [**6**][pts], M′ = Pt); $[(\eta^5\text{-Cp}')_3Mo_3S_4Ni(AsPh_3)][pts]$ ([**7**][pts]). The compounds [**5**][pts]–[**7**][pts] are completing the extensive series of clusters $[(\eta^5\text{-Cp}')_3M_3S_4M'(EPh_3)][pts]$ (M = Mo, W; M′ = Ni, Pd, Pt; E = P, As) which allows the consequences of replacing a single type of atom on structural and NMR and UV/vis spectroscopic as well as electrochemical properties to be determined. Single-crystal X-ray structure determinations of [**5**][pts]–[**7**][pts] revealed that [**5**][pts] was not isomorphous to the other members of the series $[(\eta^5\text{-Cp}')_3M_3S_4M'(EPh_3)][pts]$ due to distinctly different cell parameters, which in the molecular structure of $[\mathbf{5}]^+$ is reflected in a slightly different orientation of the PPh_3 ligand. Electrochemical measurements on the series showed that the Mo-based clusters were more difficult to oxidize than their W-based analogues. The Pd-containing clusters underwent two-electron oxidation processes, whereas the Ni- and Pt-containing clusters underwent two separated one-electron oxidation processes.

Introduction

The chemistry of the geometrically incomplete cubane-like cluster cores $M_3S_4^{4+}$ (M = Mo, W) has been explored for more than 2 decades with respect to incorporation of a wide range of main group and transition metal atoms.[1−3] Whereas cluster compounds with some 20 different cubane-like Mo_3S_4M' cores have now been reported, preparation of W_3S_4M' cores has been more difficult. W_3S_4M' cluster cores are known only for M′ = In,[4] Ge,[4] Sn,[5] Mo,[6] Re,[7] Ni,[8] Pt,[7] and Cu.[9]

Cubane-like heterobimetallic clusters have been used as simple (bioinorganic) model systems for metalloenzymes such as e.g. nitrogenases.[10,11] Their applications as catalysts for organic reactions is largely unexplored, an exception being Mo_3S_4Pd-based systems which catalyze the addition of methanol or carboxylic acids to electron-deficient alkynes.[12−15] Our own interest in heterobimetallic sulfide

* To whom correspondence should be addressed. E-mail: knh@topsoe.dk. Tel.: +45 45272678. Fax: +45 45272999.
† Haldor Topsøe A/S.
‡ Dipartimento di Chimica dell'Università di Siena.
§ Universität Erlangen-Nürnberg.

(1) Shibahara, T. *Coord. Chem. Rev.* **1993**, *123*, 73.
(2) Hernandez-Molina, R.; Sykes, A. G. *J. Chem. Soc., Dalton Trans.* **1999**, 3137.
(3) Hidai, M.; Kuwata, S.; Mizobe, Y. *Acc. Chem. Res.* **2000**, *33*, 46.
(4) Fedin, V. P.; Sokolov, M. N.; Sykes, A. G. *J. Chem. Soc., Dalton Trans.* **1996**, 4089.
(5) Müller, A.; Fedin, V. P.; Diemann, E.; Bögge, H.; Krickemeyer, E.; Sölter, D.; Giuliani, A. M.; Barbieri, R.; Adler, P. *Inorg. Chem.* **1994**, *33*, 2243.
(6) McLean, I. J.; Hernandez-Molina, R.; Sokolov, M. N.; Seo, M.-S.; Virovets, A. V.; Elsegood, M. R. J.; Clegg, W.; Sykes, A. G. *J. Chem. Soc., Dalton Trans.* **1998**, 2557.
(7) Sokolov, M. N.; Villagra, D.; El-Hendawy, A. M.; Kwak, C.-H.; Elsegood, M. R. J.; Clegg, W.; Sykes, A. G. *J. Chem. Soc., Dalton Trans.* **2001**, 2611.
(8) Shibahara, T.; Yamamoto, T.; Sakane, G. *Chem. Lett.* **1994**, 1231.
(9) Zhan, H.-Q.; Zheng, Y.-F.; Wu, X.-T.; Lu, J.-X. *Inorg. Chem. Acta* **1989**, *156*, 277.
(10) Burgess, B. K.; Lowe, D. J. *Chem. Rev.* **1996**, *96*, 2983.
(11) Beinert, H.; Holm, R. H.; Münck, E. *Science* **1997**, *277*, 653.
(12) Murata, T.; Gao, H.; Mizobe, Y.; Nakano, F.; Motomura, S.; Tanase, T.; Yano, S.; Hidai, M. *J. Am. Chem. Soc.* **1992**, *114*, 8287.

10.1021/ic0205379 CCC: $25.00
Published on Web 01/30/2003

compounds stems from the relevance of M_3S_4M' clusters (M = Mo, W; M′ = Co, Ni) as model systems for the active sites of heterogeneous CoMo/NiMo/NiW hydrodesulfurization catalysts.[16,17]

Although in some cases the coordination of organic ligands (e.g. phosphane ligands) to cubane-like M_3S_4M' cluster cores (M = Mo, W; M′ = e.g. Pt, Cu) in organic solvents such as MeOH or CH_3CN has been reported,[18−20] most of the preparative work for these heterobimetallic systems was done in aqueous phase. Recently, however, we managed to prepare organometallic derivatives of the geometrically incomplete cubane-like M_3S_4 clusters by substituting the aqua ligands in $[(H_2O)_9M_3S_4][pts]_4 \cdot 9H_2O$ (M = Mo, W; pts = *p*-toluenesulfonate) with cyclopentadienyl ligands.[21−23] The cluster compounds thus obtained, $[(\eta^5\text{-CpR})_3Mo_3S_4][pts]$ (R = H, Me) and $[(\eta^5\text{-CpR})_3W_3S_4][pts]$ (R = Me), were used as starting materials in reactions with low-valent group 6 and 8−10 metal complexes[21−24] yielding cluster compounds with novel heterobimetallic cubane-like Mo_3S_4M' cores. In particular we prepared and characterized a series of PPh_3-substituted clusters, $[(\eta^5\text{-Cp}')_3Mo_3S_4M'(PPh_3)][pts]$ (Cp′ = methylcyclopentadienyl; [**1**][pts], M′ = Ni; [**2**][pts], M′ = Pd; [**3**][pts], M′ = Pt)[22] (see Chart 1). Single-crystal X-ray structures determined at identical conditions revealed that [**1**][pts]−[**3**][pts] crystallize with isomorphous lattice parameters and allowed a comparison of radius differences for the heterometal atoms M′ = Ni, Pd, and Pt within a complete metal triad. Covalent radii varied in the order Ni < Pt < Pd, the Pt radius being 4% smaller than the Pd radius. This is due to the "lanthanide contraction" and relativistic effects intensifying the contraction of 5d metal ions. These relativistic effects have been calculated to be most pronounced for group 10 and 11 metals Au and Pt.[25] Since experimental determinations of bond lengths in isostructural compounds by X-ray diffraction may provide important input for these discussions, we intended to broaden the data basis by preparation and structural characterization of the tungsten-based clusters $[(\eta^5\text{-Cp}')_3W_3S_4M'(PPh_3)][pts]$ ([**4**][pts], M′ = Ni;[23] [**5**][pts], M′ = Pd; [**6**][pts], M′ = Pt). Additionally, an $AsPh_3$-substituted cluster, $[(\eta^5\text{-Cp}')_3Mo_3S_4Ni(AsPh_3)][pts]$ ([**7**][pts]), was prepared.

Chart 1

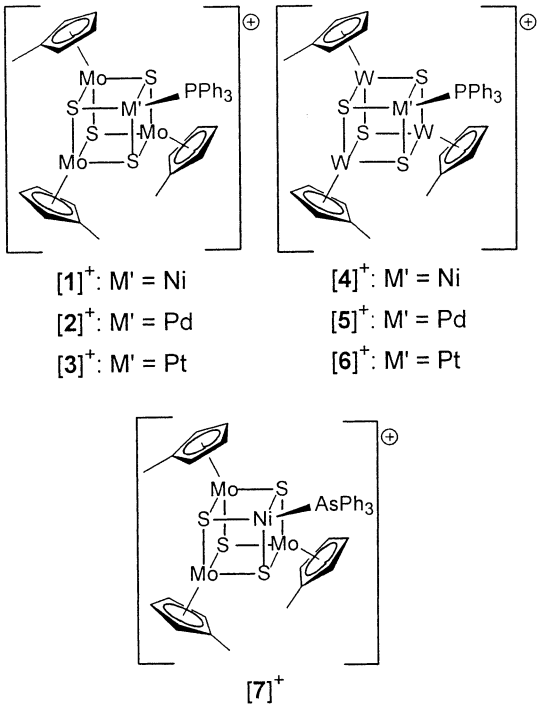

[**1**]$^+$: M′ = Ni
[**2**]$^+$: M′ = Pd
[**3**]$^+$: M′ = Pt
[**4**]$^+$: M′ = Ni
[**5**]$^+$: M′ = Pd
[**6**]$^+$: M′ = Pt
[**7**]$^+$

The cluster series [**1**][pts]−[**7**][pts] provides an unusual opportunity to study how the exchange of a single type of atoms influences the physicochemical properties within an isostructural series of compounds. This will be demonstrated by electrochemical and UV/vis spectroscopic measurements.

Experimental Section

General Procedures. All manipulations were performed under nitrogen using standard Schlenk techniques. Solvents employed were distilled from appropriate drying agents prior to use. NMR spectra: Varian UNITY 300 or Bruker DRX 600 MHz spectrometer. Residual $CHCl_3$ was used as internal reference for ^1H (7.26 ppm) and ^{13}C (77.4 ppm), while $Na_3P_3O_9$ in water was used as external reference for ^{31}P (−20.9 ppm). UV/vis spectra: Perkin-Elmer UV/vis Lambda 16 spectrometer. Elemental analyses: DB Lab, Dansk Bioprotein A/S, Odense, Denmark.

$[(H_2O)_9Mo_3S_4][pts]_4 \cdot 9H_2O$,[26] $[(H_2O)_9W_3S_4][pts]_4 \cdot 9H_2O$,[27] $[(\eta^5\text{-Cp}')_3Mo_3S_4][pts]$,[22] $[(\eta^5\text{-Cp}')_3W_3S_4][pts]$,[23] and $[Pt(nor)_3]$[28] (nor = norbornene) were prepared according to published precedures. $[Pd_2(dba)_3]$ (dba = dibenzylideneacetone) was purchased from Aldrich, and $[Ni(cod)_2]$ (cod = 1,5-cyclooctadiene) from Strem Chemicals.

Syntheses. $[(\eta^5\text{-Cp}')_3W_3S_4Pd(PPh_3)][pts]$ ([5][pts]). To a solution of $[(\eta^5\text{-Cp}')_3W_3S_4][pts]$ (77 mg, 0.071 mmol) in CH_2Cl_2 (10 mL) was added a solution of 33 mg (0.036 mmol) $[Pd_2(dba)_3]$ in CH_2Cl_2 (5 mL). The color of the nonturbid solution changed instantly from violet to yellow-brown. After the solution was stirred for 30 min at room temperature, solid PPh_3 (30 mg, 0.114 mmol) was added and the mixture stirred for an additional 1 h. The solvent was evaporated by means of vacuum. The residue was dissolved in THF (10 mL) and the solution stirred for some minutes, until a crystalline solid precipitated. Precipitation was completed by addition of pentane (10 mL). The solid was isolated by filtration,

(13) Murata, T.; Mizobe, Y.; Gao, H.; Ishii, Y.; Wakabayashi, T.; Nakano, F.; Tanase, T.; Yano, S.; Hidai, M.; Echizen, I.; Nanikawa, H.; Motomura, S. *J. Am. Chem. Soc.* **1994**, *116*, 3389.
(14) Wakabayashi, T.; Ishii, Y.; Murata, T.; Mizobe, Y.; Hidai, M. *Tetrahedron Lett.* **1995**, *36*, 5585.
(15) Wakabayashi, T.; Ishii, Y.; Ishikawa, K.; Hidai, M. *Angew. Chem.* **1996**, *108*, 2268.
(16) Riaz, U.; Curnow, O. J.; Curtis, M. D. *J. Am. Chem. Soc.* **1994**, *116*, 4357.
(17) Herbst, K.; Monari, M.; Brorson, M. *Inorg. Chem.* **2002**, *41*, 1336.
(18) Masui, D.; Ishii, Y.; Hidai, M. *Bull. Chem. Soc. Jpn.* **2000**, *73*, 931.
(19) Estevan, E.; Feliz, M.; Llusar, R.; Mata, J. A.; Uriel, S. *Polyhedron* **2001**, *20*, 527.
(20) Feliz, M.; Garriga, J. M.; Llusar, R.; Uriel, S.; Humphrey, M. G.; Lucas, N. T.; Samoc, M.; Luther-Davies, B. *Inorg. Chem.* **2001**, *40*, 6132.
(21) Rink, B.; Brorson, M.; Scowen, I. J. *Organometallics* **1999**, *18*, 2309.
(22) Herbst, K.; Rink, B.; Dahlenburg, L.; Brorson, M. *Organometallics* **2001**, *20*, 3655.
(23) Herbst, K.; Dahlenburg, L.; Brorson, M. *Inorg. Chem.* **2001**, *40*, 1989.
(24) Herbst, K.; Monari, M.; Brorson, M. *Inorg. Chem.* **2001**, *40*, 2979.
(25) Kaltsoyannis, N. *J. Chem. Soc., Dalton Trans.* **1997**, 1.
(26) Shibahara, T.; Akashi, H. *Inorg. Synth.* **1992**, *29*, 260.
(27) Shibahara, T.; Yamasaki, M.; Sakana, G.; Minami, K.; Yabuki, T.; Ichimura, A. *Inorg. Chem.* **1992**, *31*, 640.
(28) Crascall, L. E.; Spencer, J. L. *Inorg. Synth.* **1990**, *28*, 126.

washed with pentane, and dried in a vacuum. Yield: 95 mg (0.065 mmol, 92%).

^{1}H NMR ($CDCl_3$, δ/ppm): 2.30 (s, 3 H, pts); 2.33 (s, 9 H, Cp′); 5.73 (t, J = 2.4 Hz, 6 H, Cp′); 5.77 (t, 6 H, Cp′); 7.11 (d, J = 8.1 Hz, 2 H, pts); 7.16 (dd, J = 7.1 + 1.6 Hz, 6 H, PPh_3); 7.31 (t, J = 7.3 Hz, 6 H, PPh_3); 7.37 (t, 3 H, PPh_3); 7.85 (d, 4 H, pts). ^{13}C{^{1}H} NMR ($CDCl_3$, δ/ppm): 16.0 (s, Cp′); 21.7 (s, pts); 92.1 (s, Cp′); 126.2 (s, pts); 127.7 (s, PPh_3); 128.6 (s, pts); 130.2 (s, PPh_3); 133.7 (s, PPh_3). ^{31}P{^{1}H} NMR ($CDCl_3$, δ/ppm): 7.5 (s). UV/vis (MeOH; λ_{max}/nm (ϵ/dm^3 mol^{-1} cm^{-1})): 276 (26 000); 436 (5500). Anal. Calcd for $C_{43}H_{43}O_3PPdS_5W_3$ (M_r = 1457.06): C, 35.45; H, 2.97; S, 11.00. Found: C, 35.95; H, 3.10; S, 11.00.

[(η^5-Cp′)$_3$W$_3$S$_4$Pt(PPh$_3$)][pts] ([6][pts]). To a solution of [(η^5-Cp′)$_3$W$_3$S$_4$][pts] (86 mg, 0.079 mmol) in methanol (10 mL) was added a solution of 38 mg (0.080 mmol) [Pt(nor)$_3$] in CH_2Cl_2 (2 mL). The color of the nonturbid solution changed instantly from violet to brown. After the solution was stirred for 30 min at room temperature, solid PPh_3 (30 mg, 0.114 mmol) was added. The mixture was heated to reflux for 1 h. After cooling, the solvent was evaporated by means of vacuum. The brown-green residue was dissolved in THF (10 mL) and worked up in the same way as described for [**5**][pts]. Yield: 107 mg (0.69 mmol, 88%).

^{1}H NMR ($CDCl_3$, δ/ppm): 2.30 (s, 3 H, pts); 2.35 (s, 9 H, Cp′); 5.60 (t, J = 2.5 Hz, 6 H, Cp′); 5.73 (t, 6 H, Cp′); 7.10 (d, J = 7.7 Hz, 2 H, pts); 7.20 (dd, J = 7.9 + 1.9 Hz, 6 H, PPh_3); 7.32 (t, J = 7.4 Hz, 6 H, PPh_3); 7.38 (t, 3 H, PPh_3); 7.86 (d, 4 H, pts). ^{13}C{^{1}H} NMR ($CDCl_3$, δ/ppm): 15.8 (s, Cp′); 21.7 (s, pts); 90.8 (s, Cp′); 91.0 (s, Cp′); 126.5 (s, pts); 128.6 (s, PPh_3); 128.6 (s, pts); 129.9 (s, PPh_3); 134.0 (s, PPh_3). ^{31}P{^{1}H} NMR ($CDCl_3$, δ/ppm): 0.9 (s, ^1J(PtP) = 7276 Hz). UV/vis (MeOH; λ_{max}/nm (ϵ/dm^3 mol^{-1} cm^{-1})): 261 (23 200); 421 (3900). EI$^+$ mass spectrum (m/z): 1375 (M$^+$ − pts). Anal. Calcd for $C_{43}H_{43}O_3PPtS_5W_3$ (M_r =1545.73): C, 33.41; H, 2.80; S, 10.37. Found: C, 33.17; H, 3.04; S, 10.36.

[(η^5-Cp′)$_3$Mo$_3$S$_4$Ni(AsPh$_3$)][pts] ([7][pts]). To a solution/suspension of 115 mg (0.139 mmol) [(η^5-Cp′)$_3$Mo$_3$S$_4$][pts] in THF (20 mL) was added a solution/suspension of 38.3 mg (0.139 mmol) [Ni(cod)$_2$] in THF (5 mL). The mixture was stirred for 15 min, until a brown solution had formed. $AsPh_3$ (42.7 mg, 0.139 mmol) was added, which caused precipitation of a red-brown, microcrystalline solid. After 2 h of stirring, pentane (10 mL) was added. The solid was isolated by filtration, washed with pentane, and dried in a vacuum. From the filter, the solid was extracted with CH_2Cl_2 (2 × 5 mL). Pentane (20 mL) was added to the filtrate causing precipitation of [**7**][pts] as a red-brown solid. This was collected on a filter, washed with pentane, and dried in a vacuum. Yield: 143 mg (0.120 mmol, 86%).

^{1}H NMR ($CDCl_3$, δ/ppm): 2.04 (s, 9 H, Cp′); 2.29 (s, 3 H, pts); 5.53 (t, J = 2.4 Hz, 6 H, Cp′); 5.62 (t, 6 H, Cp′); 7.08 (d, J = 7.8 Hz, 2 H, pts); 7.20 (m, 6 H, PPh_3); 7.39 (m, 9 H, PPh_3); 7.85 (d, 2 H, pts). FAB$^+$ mass spectrum (m/z (% abundance)): 1018 (M$^+$ − pts, 62); 712 (M$^+$ − pts − $AsPh_3$, 100); 633 (M$^+$ − pts −$AsPh_3$ − Cp′, 20). UV/vis (MeOH; λ_{max}/nm (ϵ/dm^3 mol^{-1} cm^{-1})): 279 (17 300); 522 (1100); 683 (600). Anal. Calcd for $C_{43}H_{43}AsMo_3NiO_3S_5$ (M_r = 1189.55): C, 43.42; H, 3.64; S, 13.48. Found: C, 43.45; H, 3.87; S, 14.22.

X-ray Crystallography. X-ray data for [**5**][pts], [**6**][pts], and [**7**][pts] were collected on a Nonius MACH 3 diffractometer using graphite-monochromated Mo Kα radiation (0.710 73 Å). The structures were solved by direct methods (SIR-97[29]) and subsequently refined by full-matrix least-squares procedures on F^2 with allowance for anisotropic thermal motion of all non-hydrogen atoms employing the WinGX[30] package and the relevant programs (SHELXL-97,[31] ORTEP-3[32]) implemented therein. H atoms were included in the final structural models by assuming ideal geometry and using appropriate riding models.

Electrochemistry. Materials and apparatus for electrochemistry have been described elsewhere.[33] All the potential values are referred to the saturated calomel electrode. Under the present experimental conditions the one electron oxidation occurs at $E^{\circ\prime}$ = +0.40 V vs SCE.

Table 1. Comparison of ^{31}P{^{1}H} NMR Spectroscopic Data for [**1**][pts]−[**6**][pts]

	δ/ppm (^1J(PtP)/Hz)	
cluster core	M = Mo	M = W
M_3S_4Ni	34.4[a]	12.7[b]
M_3S_4Pd	26.6[a]	7.5[c]
M_3S_4Pt	15.4 (6656)[a]	0.9 (7276)[c]

[a] Reference 22. [b] Reference 23. [c] This work.

Results and Discussion

Synthesis. The heterobimetallic cluster compounds [**5**][pts] and [**6**][pts] (Chart 1) were prepared by subsequent addition of a metal alkene complex and PPh_3 to solutions of the homometallic starting material [(η^5-Cp′)$_3$W$_3$S$_4$][pts]. The reaction between [(η^5-Cp′)$_3$W$_3$S$_4$][pts] and [Pd$_2$(dba)$_3$] (molar ratio W:Pd = 3:1) in CH_2Cl_2 resulted in an instant color change of the mixture from violet to yellow-brown. This indicated an immediate scission of the Pd−dba bonds and the incorporation of the Pd atom into the W_3S_4 cluster core, which may be viewed as a tridentate macrocyclic ligand coordinating to the Pd atom. After incorporation of the Pd atom into the tungsten cluster, a PPh_3 ligand was coordinated to the fourth coordination site at the Pd atom. From THF/pentane, [(η^5-Cp′)$_3$W$_3$S$_4$Pd(PPh$_3$)][pts] ([**5**][pts]) was isolated as a brown powder. A similar preparative procedure was applied for the reaction between [(η^5-Cp′)$_3$W$_3$S$_4$][pts] and [Pt(nor)$_3$] in methanol solution. After addition of PPh_3 the mixture was heated to reflux to ensure complete substitution of the norbornene ligands by PPh_3. [(η^5-Cp′)$_3$W$_3$S$_4$Pt(PPh$_3$)][pts] ([**6**][pts]) was isolated as a brown-green powder.

The preparation of [(η^5-Cp′)$_3$Mo$_3$S$_4$Ni(AsPh$_3$)][pts] ([**7**][pts]) was carried out in THF in which both starting materials, [(η^5-Cp′)$_3$Mo$_3$S$_4$][pts] and [Ni(cod)$_2$], were only slightly soluble. However, mixing THF suspensions of [(η^5-Cp′)$_3$Mo$_3$S$_4$][pts] and [Ni(cod)$_2$], respectively, resulted in the formation of a brown solution. Addition of $AsPh_3$ produced a microcrystalline precipitate which, by recrystallization from CH_2Cl_2/pentane, gave a red-brown powder of [**7**][pts].

A comparison of ^{31}P{^{1}H} NMR spectroscopic data within the series [**1**][pts]−[**6**][pts] (Table 1) shows that the signals for the tungsten-based cluster compounds [**4**][pts]−[**6**][pts]

(29) Altomare, A.; Burla, M. C.; Camalli, M.; Cascarano, G. L.; Giacovazzo, C.; Guagliardi, A.; Moliterni, A. G. G.; Polidori, G.; Spagna, R. *J. Appl. Crystallogr.* **1999**, *32*, 115.

(30) Farrugia, L. J. *J. Appl. Crystallogr.* **1999**, *32*, 837.

(31) Sheldrick, G. M. *SHELXL-97-A Program for the Refinement of Crystal Structures from Diffraction Data (Release 97-2)*; Universität Göttingen: Göttingen, Germany, 1997.

(32) Farrugia, L. J. *J. Appl. Crystallogr.* **1997**, *30*, 565.

(33) Zanello, P.; Laschi, F.; Fontani, M.; Mealli, C.; Ienco, A.; Tang, K.; Jin, X.; Li, L. *J. Chem. Soc., Dalton Trans.* **1999**, 965.

Table 2. UV/Vis Spectroscopic Data for [**1**][pts]−[**6**][pts]

cluster core	$\lambda_{max/nm}$ (ϵ/L·mol^{-1}·cm^{-1}) M = Mo	M = W
$[(\eta^5\text{-Cp}')_3M_3S_4Ni(PPh_3)]^+$	286 (24 300)[a] 513 (1900)	267 (18 200)[b] 479 (1500)
$[(\eta^5\text{-Cp}')_3M_3S_4Pd(PPh_3)]^+$	291 (27 700)[a] 472 (5600)	276 (26 000)[c] 436 (5500)
$[(\eta^5\text{-Cp}')_3M_3S_4Pt(PPh_3)]^+$	287 (23 600)[a] 451 (3900)	261 (23 200)[c] 421 (3900)

[a] Reference 22. [b] Reference 23. [c] This work.

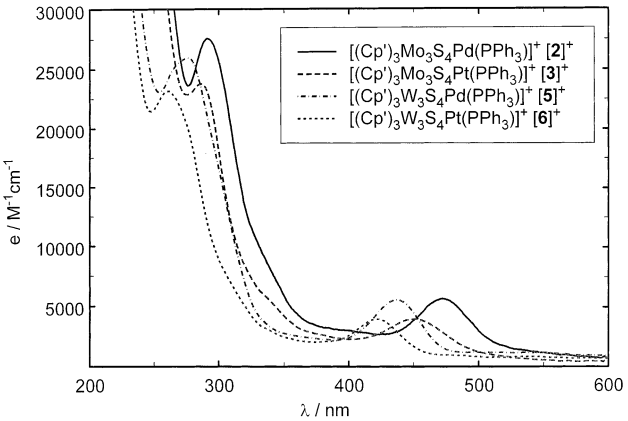

Figure 1. UV/vis spectra of $[(\eta^5\text{-Cp}')_3Mo_3S_4M'(PPh_3)]$[pts] ([**2**][pts], M′ = Pd; [**3**][pts], M′ = Pt)[21] and $[(\eta^5\text{-Cp}')_3W_3S_4M'(PPh_3)]$[pts] ([**5**][pts], M′ = Pd; [**6**][pts], M′ = Pt) in methanol.

are shifted by ca. 20 ppm to higher field than the resonances of their molybdenum-based counterparts. The highfield shift indicates an increase of electron density at the phosphorus atom caused by the electron-rich tungsten atoms. For [**6**][pts], a coupling constant ^1J(PtP) of 7276 Hz was observed. This large value is out of range for coupling constants $^1J(Pt^{II}P)$, which are reported to lie between 1400 and 5000 Hz.[34] Phosphorus couplings to zerovalent platinum $^1J(Pt^0P)$, however, can range up to 9000 Hz, which supports the view that the heterometal is Pt^0-like rather than Pt^{II}-like.

Table 2 gives positions and intensities of the absorption bands in the UV/vis spectrum for the series [**1**]$^+$−[**6**]$^+$. The UV/vis spectra of the Pd-containing cluster pair [**2**]$^+$/[**5**]$^+$ and the Pt-containing cluster pair [**3**]$^+$/[**6**]$^+$ are displayed in Figure 1. Each spectrum shows two charge-transfer bands: a high-intensity band below 300 nm and a band with medium intensity in the visible region above 400 nm. For this set of bands, the consequences of replacing a single type of atom in a cubane-like cluster are clearly demonstrated. Going from Mo to W causes a blue-shift by 15−26 nm for the high-intensity band below 300 nm and 30−36 nm for the band in the visible region. A similar hypsochromic shift for Mo/W-containing clusters was recently found for the heterobimetallic cluster anions $[\{(OC)_3Re\}_3S_4M(S)]^-$ (M = Mo, W) and was ascribed to the stronger electron-accepting ability of molybdenum compared to tungsten.[35] A blue-shift of the absorption band in the visible region is also detected when going down the Ni triad. Replacing Ni by Pd causes this band to shift by 41−43 nm, whereas going from Pd to Pt only causes a shift of 15−21 nm. This pattern is also reflected in the colors of the clusters, which range from red ([**1**][pts]) to yellow-brown ([**5**][pts]) to green-brown ([**6**][pts]).

A comparison between the UV/vis spectra of the Mo_3S_4-Ni clusters [**1**]$^+$ and [**7**]$^+$ shows that the replacement of the PPh_3 ligand by an $AsPh_3$ ligand has only minor, but opposite, consequences on the two UV/vis band positions. Whereas the high-intensity charge-transfer band undergoes a 7 nm blue-shift by replacing PPh_3 by $AsPh_3$, the band in the visible region undergoes a 9 nm red-shift.

Crystallography. X-ray crystal structures of [**5**][pts]−[**7**]-[pts] were determined at experimental conditions identical with those of [**1**][pts]−[**4**][pts] to ensure full comparability of all structural parameters. Details for the structure determinations are given in Table 3. The cluster cations [**5**]$^+$ and [**7**]$^+$ are depicted in Figures 2 and 3, and selected bond lengths and angles are listed in Tables 4 and 5.

In a qualitative description, the cluster cores of [**5**]$^+$ and [**6**]$^+$ consist of a slightly distorted tetrahedral arrangement of one palladium or platinum and three tungsten atoms. Each tetrahedral face is capped by a μ_3-coordinated sulfido ligand thus generating a cubane-like structure. The coordination sphere of each W atom is completed by a Cp′ ligand, whereas the heterometals Pd or Pt coordinate additionally to three sulfido ligands one PPh_3 ligand. The W−W distances in both cluster cations (in [**5**]$^+$, 2.7961(8)−2.8124(8) Å; in [**6**]$^+$, 2.8215(11)−2.8287(11) Å) are consistent with the presence of metal−metal bonds. Due to the positive charge of [**6**]$^+$ the W−Pt distances (2.8935(11)−2.9109(10) Å) are slightly longer than the W−Pt bond lengths found in the trinuclear cluster $[(Et_2NCS_2)_2W_2S_4Pt(PPh_3)]$ (2.787(1) and 2.796(1) Å).[36] In fact, the W−Pt distances are at the upper limit of known W−Pt bond lengths (2.663−2.895 Å).[37]

A very similar description as for the tungsten-based clusters [**5**]$^+$ and [**6**]$^+$ can be given for $[(\eta^5\text{-Cp}')_3Mo_3S_4Ni(AsPh_3)]^+$ ([**7**]$^+$) whose innermost metallic core consists of a tetrahedral framework of one nickel atom and three molybdenum atoms. Again, a sulfido ligand is capping each tetrahedral face which leads to the formation of a cubane-like cluster core. The Mo−Mo and Mo−Ni distances are consistent with the presence of metal−metal single bonds. Thus, with six metal−metal bonds in each cluster core, the cluster cations [**5**]$^+$−[**7**]$^+$ constitute electron-precise 60 VE clusters according to Mingos' and Wade's polyhedral skeletal electron pair theory.[38]

However, an inspection of the structural parameters within the cluster series [**1**]$^+$−[**7**]$^+$ shows that the W/Pd cluster [**5**]$^+$ is not isomorphous to the other compounds of this series. Although crystallized at the same conditions (combination

(34) Verkade, J. G.; Mosbo, J. A. In *Methods in Stereochemical Analysis*; Marchand, A. P., Ed.; VCH Publishers: Deerfield Beach, FL, 1987; Vol. 8, Chapter 13, pp 425−464.
(35) Hornung, F.; Wanner, M.; Klinkhammer, K. W.; Kaim, W.; Fiedler, J. *Z. Anorg. Allg. Chem.* **2001**, *627*, 2430.
(36) Ikada, T.; Kuwata, S.; Mizobe, Y.; Hidai, M. *Inorg. Chem.* **1998**, *37*, 5793.
(37) Bender, R.; Braunstein, P.; Jud, J.-M.; Dusausoy, Y. *Inorg. Chem.* **1984**, *23*, 4489.
(38) Mingos, D. M. P.; Wales, D. J. In *Introduction to Cluster Chemistry*; Grimes, R. N., Ed.; Prentice Hall Inorganic and Organometallic Chemistry Series; Prentice Hall: Englewood Cliffs, NJ, 1990; p 72 ff.

Table 3. Crystal and Refinement Data for $[(\eta^5\text{-Cp}')_3W_3S_4M'(PPh_3)][pts]$ ([**5**][pts], M′ = Pd; [**6**][pts], M′ = Pt) and $[(\eta^5\text{-Cp}')_3Mo_3S_4Ni(AsPh_3)][pts]$ ([**7**][pts])

	[**5**][pts]	[**6**][pts]	[**7**][pts]
chem formula	$C_{43}H_{43}O_3PPdS_5W_3$	$C_{43}H_{43}O_3PPtS_5W_3$	$C_{43}H_{43}AsMo_3NiO_3S_5$
fw	1456.99	1545.68	1189.52
space group	$P2_1/n$ (No.14)	$P2_1/n$ (No.14)	$P2_1/n$ (No.14)
a (Å)	11.229(1)	9.449(2)	9.484(1)
b (Å)	24.098(3)	10.811(2)	10.877(1)
c (Å)	16.457(5)	42.900(8)	42.327(4)
β (deg)	95.70(1)	92.51(2)	92.10(1)
V (Å^3)	4431.2(15)	4378.2(15)	4363.5(7)
Z	4	4	4
T (K)	293(2)	293(2)	293(2)
λ (Å)	0.710 73	0.710 73	0.710 73
D_c (g cm^{-3})	2.184	2.345	1.811
μ (mm^{-1})	8.472	11.355	2.298
$R(F_o)^a$	0.1029	0.1084	0.0970
$R_w(F_o^2)^b$	0.1133	0.1441	0.0885

^{a} $R = \sum||F_o| - |F_c||/\sum|F_o||$. ^{b} $R_w = [\sum w(F_o^2 - F_c^2)^2/\sum w(F_o^2)^2]^{1/2}$, where $w = 1/[\sigma^2(F_o^2) + (aP)^2 + bP]$ and where $P = (F_o^2 + 2F_c^2)/3$.

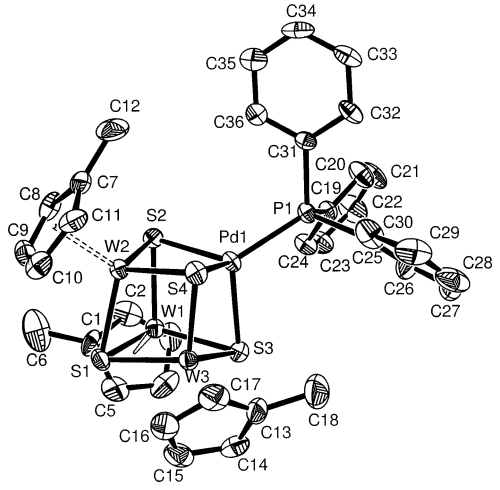

Figure 2. ORTEP plot of the cluster cation $[(\eta^5\text{-Cp}')_3W_3S_4Pd(PPh_3)]^+$ ($[\mathbf{5}]^+$). Atoms are drawn at the 30% probability level. Hydrogen atoms have been removed for clarity.

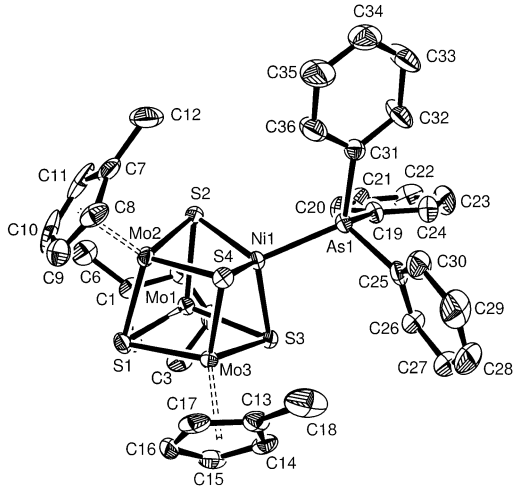

Figure 3. ORTEP plot of the cluster cation $[(\eta^5\text{-Cp}')_3Mo_3S_4Ni(AsPh_3)]^+$ ($[\mathbf{7}]^+$). Atoms are drawn at the 30% probability level. Hydrogen atoms have been removed for clarity.

of solvents, temperature), its lattice parameters are distinctly different from those of the rest of the series. In the isostructural series [**1**][pts]−[**4**][pts] and [**6**][pts] and [**7**][pts], the PPh_3 ligand coordinates to the heterometal in a characteristic "oblique" position with respect to the heterometal−S(1) axis, presumably caused by two Cp′ methyl groups which point toward the phenyl rings. This "oblique" position is expressed by a large scattering of the S−M′−P angles (e.g., the S−Pd−P angles in $[\mathbf{2}]^+$ vary between 108.55(5) and 122.64(5)°). For the nonisomorphous compound [**5**][pts], however, this range is much smaller (113.75(13)−119.73(12)°) and the PPh_3 ligand coordinates almost symmetrically with respect to the Pd(1)−S(1) axis.

A particular reason for the structure determinations of [**5**][pts] and [**6**][pts] was to obtain information for a comparison

Table 4. Selected Bond Lengths (Å) and Angles (deg) for $[(\eta^5\text{-Cp}')_3W_3S_4M'(PPh_3)][pts]$ ([**5**][pts], M′ = Pd; [**6**][pts], M′ = Pt)

	[**5**][pts] (M′ = Pd)	[**6**][pts] (M′ = Pt)
W(1)−W(2)	2.7961(8)	2.822(1)
W(1)−W(3)	2.8124(8)	2.829(1)
W(2)−W(3)	2.8071(8)	2.822(1)
W(1)−M′	2.914(1)	2.894(1)
W(2)−M′	2.917(1)	2.911(1)
W(3)−M′	2.899(1)	2.899(1)
M′−S(2)	2.400(4)	2.395(5)
M′−S(3)	2.409(4)	2.395(5)
M′−S(4)	2.399(4)	2.393(4)
M′−P(1)	2.282(3)	2.217(4)
W(1)−M′−W(2)	57.30(2)	58.17(3)
W(1)−M′−W(3)	57.87(3)	58.46(3)
W(2)−M′−W(3)	57.72(2)	58.11(3)
W(1)−M′−P(1)	150.00(10)	138.73(13)
W(2)−M′−P(1)	144.57(9)	143.91(13)
W(3)−M′−P(1)	143.73(10)	153.45(13)
S(2)−M′−S(3)	100.08(12)	101.31(16)
S(2)−M′−S(4)	99.76(12)	100.81(15)
S(3)−M′−S(4)	101.24(13)	101.24(15)
S(2)−M′−P(1)	119.73(12)	109.30(16)
S(3)−M′−P(1)	119.00(12)	117.70(16)
S(4)−M′−P(1)	113.75(13)	123.25(16)

Table 5. Selected Bond Lengths (Å) and Angles (deg) for $[(\eta^5\text{-Cp}')_3Mo_3S_4Ni(AsPh_3)][pts]$ ([**7**][pts])

Mo(1)−Mo(2)	2.8291(8)	Mo(1)−Ni(1)	2.7031(9)
Mo(1)−Mo(3)	2.8319(8)	Mo(2)−Ni(1)	2.7010(9)
Mo(2)−Mo(3)	2.8382(8)	Mo(3)−Ni(1)	2.6940(9)
Ni(1)−S(2)	2.1970(17)	Ni(1)−S(4)	2.2088(18)
Ni(1)−S(3)	2.2016(18)	Ni(1)−As(1)	2.2552(10)
Mo(1)−Ni(1)−Mo(2)	63.14(2)	S(2)−Ni(1)−S(3)	107.97(7)
Mo(1)−Ni(1)−Mo(3)	63.30(2)	S(2)−Ni(1)−S(4)	108.42(7)
Mo(2)−Ni(1)−Mo(3)	63.48(2)	S(3)−Ni(1)−S(4)	108.51(7)
Mo(1)−Ni(1)−As(1)	140.86(4)	S(2)−Ni(1)−As(1)	116.97(6)
Mo(2)−Ni(1)−As(1)	150.45(4)	S(3)−Ni(1)−As(1)	103.03(5)
Mo(3)−Ni(1)−As(1)	135.62(4)	S(4)−Ni(1)−As(1)	111.50(6)

Table 6. Comparison of M′−P(1) Distances in $[\mathbf{1}]^+$−$[\mathbf{6}]^+$

compd/metals M−M′	dist M′−P(1) (Å)	diff (Å)	ref
$[\mathbf{1}]^+$/Mo−Ni	2.160(2)	−0.017	22
$[\mathbf{4}]^+$/W−Ni	2.143(3)		23
$[\mathbf{2}]^+$/Mo−Pd[a]	2.277(1)	+0.005	22
$[\mathbf{5}]^+$/W−Pd[a]	2.282(3)		this work
$[\mathbf{3}]^+$/Mo−Pt	2.232(4)	−0.015	22
$[\mathbf{6}]^+$/W−Pt	2.217(4)		this work

[a] Compounds not isostructural.

of the Pd−P and Pt−P distances in these clusters, as we previously did for the Mo-based clusters [**2**][pts] and [**3**][pts]. However, as outlined by Schmidbaur in a discussion of covalent radius differences between Ag and Au atoms, comparable complexes must have identical coordination spheres both for ligands and counterions and must crystallize in isomorphous lattices determined at identical experimental conditions.[39] For [**5**][pts], the criterion of isomorphism with [**6**][pts] (and the other compounds in this series, [**1**][pts]−[**4**][pts] and [**7**][pts]) is clearly not fulfilled. For this reason, a comparison between the Pd−P and Pt−P bonds in $[\mathbf{5}]^+$ and $[\mathbf{6}]^+$ could not be carried out as intended.

The comparison of M′−P(1) distances within the isostructural Mo/W cluster pairs $[\mathbf{1}]^+/[\mathbf{4}]^+$ (Ni−P bonds) and $[\mathbf{3}]^+/[\mathbf{6}]^+$ (Pt−P bonds) shows that these distances are reduced by ca. 0.015−0.017 Å in the W-based cluster cores (Table 6). Since structural reasons are not responsible for this effect, the electron distribution within the W_3S_4M' cluster cores presumably causes these bond length reductions. In the nonisostructural cluster pair $[\mathbf{2}]^+/[\mathbf{5}]^+$ (Pd−P bonds), this effect is not seen and, in fact, the Pd(1)−P(1) distance in W-based $[\mathbf{5}]^+$ is slightly longer than in Mo-based $[\mathbf{2}]^+$.

The cluster compound [**5**][pts] constitutes the first example of a cluster with a W_3S_4Pd core. Whereas the clusters $[(H_2O)_9Mo_3S_4][pts]_4$ and $[(H_2O)_9W_3S_4][pts]_4$ show marked differences in their reactivities toward palladium black in aqueous solution,[40] the organometallic cluster $[(\eta^5\text{-Cp}')_3W_3S_4]$[pts] behaves completely analogous to its Mo counterpart $[(\eta^5\text{-Cp}')_3Mo_3S_4]$[pts]. This makes the $[(\eta^5\text{-Cp}')_3W_3S_4]$[pts] cluster a convenient starting material for the incorporation of further transition metals. The incorporation of group 6, 8, and 9 metals into the cluster core of $[(\eta^5\text{-Cp}')_3Mo_3S_4]$[pts] has already been demonstrated.[21,24]

A comparison of the $AsPh_3$-substituted cluster cation $[\mathbf{7}]^+$ to its PPh_3 substituted analogue $[\mathbf{1}]^+$ shows almost identical distances and angles for both Mo_3S_4Ni cluster cores. The largest difference is found in the Mo−Ni distances which are slightly shorter in $[\mathbf{7}]^+$ (range: 2.6940(9)−2.7031(9) Å) than in $[\mathbf{1}]^+$ (range: 2.7088(8)−2.7237(8) Å). This reduction of metal−metal distances in $[\mathbf{7}]^+$ is due to the softer donor properties of the $AsPh_3$ ligand compared to PPh_3, which the Ni atom compensates by shorter distances to its other binding partners.

Electrochemistry. Electrochemical characterization of homo- and heterometallic sulfur cluster compounds has previously been undertaken in a number of cases.[41,42] Cyclic voltamograms of $[Mo_3S_4(ida)_3]^{2-}$ (H_2ida = iminodiacetic acid),[43] $[M_3S_4(Hnta)_3]^{2-}$ (M = Mo, W; H_3nta = nitrilotriacetic acid),[44] and $[Mo_3S_4(H_2O)_9]^{4+}$ [45] all reveal the presence of 3 reduced cluster states. Apart from the reduction to the most reduced state, $Mo^{IV}Mo^{III}_2 \rightarrow Mo^{III}_3$, these redox processes are all reversible. The CV of $[Mo_3S_4Cl_3(dmpe)_3]^+$ (dmpe = 1,2-bis(dimethylphosphino)ethane) displays two quasi-reversible one-electron reductions;[46] for the tungsten analogue, $[W_3S_4Cl_3(dmpe)_3]^+$, one quasi-reversible reduction involving an unknown number of electrons is seen.[46]

Formal electrode potentials for all redox changes for the members of the extensive series [**1**][pts]−[**7**][pts] are found in Table 7. Figure 4 shows the cyclic voltammetric behavior of the W_3NiS_4 monocation $[\mathbf{4}]^+$ in dichloromethane solution. It undergoes one reduction as well as two separated oxidation processes, all displaying features of chemical reversibility in the cyclic voltammetric time scale. A further irreversible oxidation is seen at higher potential (better resolved at the glassy carbon electrode; $E_p = +1.41$ V), and this is assigned to the oxidation of the coordinated triphenylphosphine. On the basis of the relative peak heights, it is conceivable that all the reversible processes involve the same number of electrons on the cyclic voltammetric time scale. Attempts to determine such a number of electrons by controlled potential coulometry in correspondence to the first oxidation ($E_w = +0.7$ V) failed because of slow poisoning electrode effects, which prevented completion of the measurement; after the consumption of a number of electrons $n_{app} \approx 0.3$ the electrolysis current slows down and the resulting cyclic voltammetric profile remains essentially unaltered. Nevertheless, addition of a proper calibrant as an internal standard (namely, the bis(boronium ferrocenyl) derivative $Fc_2(FeB_2C_{54}N_{12}H_{42})$, $M_r = 1222$, which undergoes an initial one-electron oxidation followed by a two-electron oxidation ($E^{\circ\prime}_{0/+} = +0.28$ V; $E^{\circ\prime}_{+/3+} = +0.61$ V)[47]) confirmed the one-electron nature of each redox step exhibited by $[\mathbf{4}]^+$. Analysis of both the first anodic and the cathodic responses with scan rate varying from 0.02 to 2 V s^{-1} confirmed their chemical and electrochemical reversibility in that (i) the $i_{p(backward)}/i_{p(forward)}$ response is constantly equal to 1, (ii) the peak-to-peak separation maintains close to the theoretical value of 60 mV, and (iii) the current function $i_{p(forward)}\upsilon^{-1/2}$ is substantially constant.

Figure 5 shows the cyclic voltammetric patterns exhibited by the monocations $[\mathbf{5}]^+$ (M′ = Pd; Figure 5a) and $[\mathbf{6}]^+$ (M′ = Pt; Figure 5b). Stated the constant presence of the reversible one-electron reduction, the platinum complex $[\mathbf{6}]^+$ undergoes two separated one-electron oxidations, the first of which is partially chemically reversible (for instance, the

(39) Bayler, A.; Schier, A.; Bowmaker, G. A.; Schmidbaur, H. *J. Am. Chem. Soc.* **1996**, *118*, 7006.
(40) Fedin, V. P.; Seo, M.-S.; Saysell, D. M.; Dybtsev, D. N.; Elsegood, M. R. J.; Clegg, W.; Sykes, A. G. *J. Chem. Soc., Dalton Trans.* **2002**, 138.
(41) Zanello, P. *Coord. Chem. Rev.* **1988**, *83*, 199.
(42) Zanello, P. *Coord. Chem. Rev.* **1988**, *87*, 1.
(43) Shibahara, T.; Kuroya, H. *Polyhedron* **1986**, *5*, 357.
(44) Shibahara, T.; Yamasaki, M.; Sakane, G.; Minami, K.; Yabuki, T.; Ichimura, A. *Inorg. Chem.* **1992**, *31*, 640.
(45) Shibahara, T.; Sakane, G.; Naruse, Y.; Taya, K.; Akashi, H.; Ichimura, A.; Adachi, H. *Bull. Chem. Soc. Jpn.* **1995**, *68*, 2769.
(46) Cotton, F. A.; Llusar, R.; Eagle, C. T. *J. Am. Chem. Soc.* **1989**, *111*, 4332.
(47) Wagner, M.; Zanello, P. Unpublished results.

Table 7. Electrochemical Characteristics of Compounds [**1**][pts]−[**7**][pts] and Their Precursors $[(\eta^5\text{-Cp}')_3M_3S_4)]$[pts] (M = Mo, W) in Dichloromethane Solution

	$E^{o'}_{+/2+}$ (V)	$\Delta E_p{}^a$ (mV)	$i_{pc}/i_{pa}{}^b$	$E^{o'}_{2+/3+}$ (V)	$\Delta E_p{}^a$ (mV)	$i_{pc}/i_{pa}{}^b$	$E^{o'}_{+/0}$ (V)	$\Delta E_p{}^a$ (mV)	$i_{pc}/i_{pa}{}^b$
Mo_3	+1.19	80	0.4	+1.19	90	0.3	−0.81	94	1.0
W_3	+1.60	52	0.4	+1.60	52	0.4	−1.16	70	1.0
[**1**][pts]	+0.80	68	0.5	+1.4[b,e]			−1.20	76	1.0
[**2**][pts]	+0.72	186[b]	c	+0.72	186[b]	c	−1.07	60	1.0
[**3**][pts]	+0.79	90	0.3	+0.79	90	0.3	−1.16	60	1.0
[**4**][pts]	+0.57	62	1.0	+1.16	90	0.5	−1.55	70	1.0
[**5**][pts]	+0.56	200[b]	c	+0.56[c]	200[b]	c	−1.39	66	1.0
[**6**][pts]	+0.57	70	0.5	+0.98[a,d]			−1.40	68	1.0
[**7**][pts]	+0.80	92	0.4	+1.4[b,e]			−1.20	88	1.0
PPh_3	+1.26[a,d]								

[a] Measured at 0.2 V s^{-1}. [b] Measured at 0.1 V s^{-1}. [c] The return peak is almost overlapped by the reduction peak of side products (see text). [d] Peak potential for irreversible processes. [e] The cluster oxidation overlaps the phosphane oxidation.

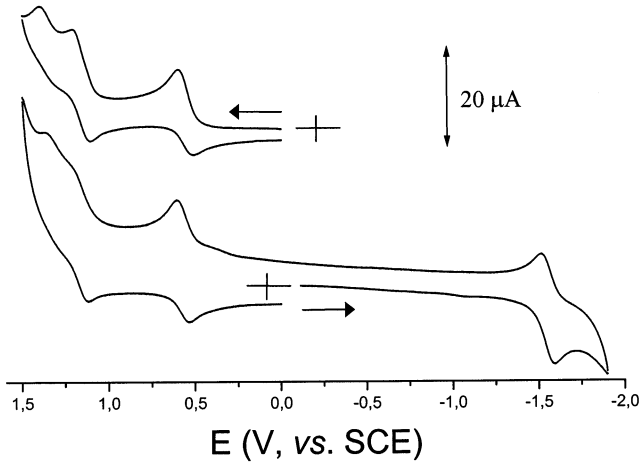

Figure 4. Cyclic voltammograms recorded on a CH_2Cl_2 solution containing $[(\eta^5\text{-Cp}')_3W_3S_4Ni(PPh_3)]^+$ [**4**]$^+$ (0.4×10^{-3} mol dm^{-3}) and $[NBu_4][PF_6]$ (0.2 mol dm^{-3}): (top) glassy carbon electrode; (bottom) platinum electrode. Scan rate: 0.2 V s^{-1}.

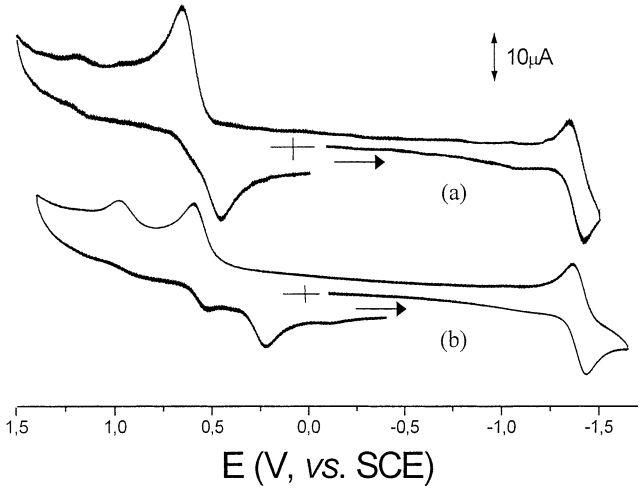

Figure 5. Cyclic voltammograms recorded at a platinum electrode on CH_2Cl_2 solutions containing $[NBu_4][PF_6]$ (0.2 mol dm^{-3}) and (a) $[(\eta^5\text{-Cp}')_3W_3S_4Pd(PPh_3)]^+$ ([**5**]$^+$) (0.4×10^{-3} mol dm^{-3}) and (b) $[(\eta^5\text{-Cp}')_3W_3S_4Pt(PPh_3)]^+$ ([**6**]$^+$) (0.4×10^{-3} mol dm^{-3}). Scan rate: 0.2 V s^{-1}.

i_{pc}/i_{pa} ratio is equal to 0.5 at 0.1 V s^{-1} and affords a secondary product which reduces at +0.2 V), whereas the second step is irreversible. In contrast, the palladium complex [**5**]$^+$ gives rise to a single two-electron anodic process, which is complicated by subsequent chemical reactions (the directly associated reduction process is almost overlapped by the major reduction peak of the byproduct which reduces at +0.5 V).

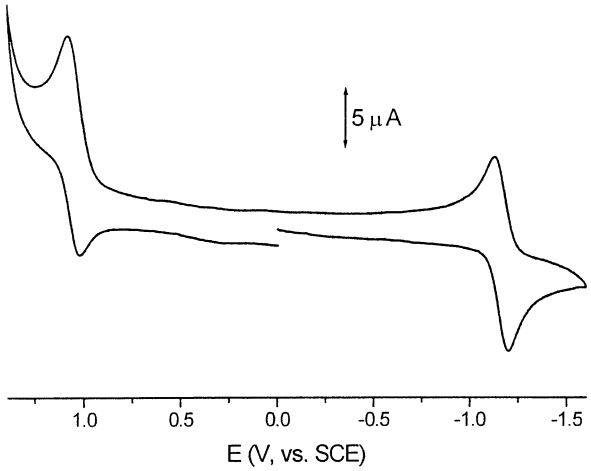

Figure 6. Cyclic voltammogram recorded at a platinum electrode on a CH_2Cl_2 solution containing $[NBu_4][PF_6]$ (0.2 mol dm^{-3}) and $[(\eta^5\text{-Cp}')_3W_3S_4)]^+$ (0.6×10^{-3} mol dm^{-3}). Scan rate: 0.2 V s^{-1}.

To understand the nature of these redox changes for [**4**]$^+$−[**6**]$^+$, the voltammetric behavior (Figure 6) of the incomplete cubane precursor $[(\eta^5\text{-Cp}')_3W_3S_4]^+$ is relevant. This cluster cation undergoes a chemically reversible one-electron reduction and a two-electron oxidation. For the anodic process, on the basis of the fact that the current ratio i_{pc}/i_{pa} decreases with the scan rate (independently from the concentration, it is equal to 0.5 at 0.05 V s^{-1} and it progressively decreases up to 0.3 at 2.00 V s^{-1}), whereas the current function remains substantially constant, we assume that a first-order reversible chemical reaction follows the partially chemically reversible two-electron removal. Unfortunately, either the closeness of the process to the solvent discharge or its incomplete chemical reversibility prevented any analysis of the species in equilibrium with the instantaneously electrogenerable trication $[(\eta^5\text{-Cp}')_3W_3S_4]^{3+}$.

If we return now to the heterometallic $[(\eta^5\text{-Cp}')_3W_3S_4M'(PPh_3)]^+$ cluster cations, it is evident that the addition of the $M'(PPh_3)$ fragment to $[(\eta^5\text{-Cp}')_3W_3S_4]^+$ simply exerts an electron-donating effect in case of the palladium complex [**5**]$^+$ with respect to $[(\eta^5\text{-Cp}')_3W_3S_4]^+$, whereas in the case of the nickel [**4**]$^+$ and platinum [**6**]$^+$ complexes more important electronic effects make the two-electron wave split into two separated one-electron processes. It could be speculated that in these latter cases an electronic communication is introduced inside the heterocubane assembly or, from

a conceptual viewpoint, the addition of the $M'(PPh_3)$ fragment to $[(\eta^5\text{-}Cp')_3W_3S_4]^+$ acts as a molecular electronic switch.[48]

From a qualitative viewpoint, the members of the molybdenum-based cluster series $[\mathbf{1}]^+-[\mathbf{3}]^+$ all give rise to a rather similar redox behavior, except for the palladium complex, which also undergoes a single two-electron oxidation. The formal electrode potentials of all the redox changes are compiled in Table 7.

Compared to the W analogues, the Mo clusters are more difficult to oxidize and more easily reducible. This likely arises from the fact that the main block $[(\eta^5\text{-}Cp')_3Mo_3S_4]^+$ more easily buffers the electronic effects from the $M'(PPh_3)$ appendix with respect to $[(\eta^5\text{-}Cp')_3W_3S_4]^+$. In addition, at variance with $[\mathbf{4}]^+$, in this case the first anodic processes of the Ni derivatives $[\mathbf{1}]^+$ and $[\mathbf{7}]^+$ are coupled to chemical complications, thus testifying that the dication $[\mathbf{4}]^{2+}$ is notably more stable than $[\mathbf{1}]^{2+}$ and $[\mathbf{7}]^{2+}$.

Conclusion. The preparation of the cluster series $[(\eta^5\text{-}Cp')_3M_3S_4M'(PPh_3)][pts]$ (M = Mo, W; M′ = Ni, Pd, Pt) and related noble metal containing clusters prepared recently[24] enables the synthesis of bimetallic sulfide materials, whose catalytic potential, e.g. in hydrotreating catalysis, is largely unexplored. Monometallic transition metal sulfides, either as pure phases[49,50] or supported on a porous carrier material,[51] have been studied thoroughly in hydrodesulfurization (HDS) of thiophene derivatives, and a reactivity pattern in form of a "volcano curve" has been recognized. On the basis of this reactivity pattern, Nørskov[52] and Topsøe[53] developed the bond energy model (BEM) which explained the periodic trends in HDS activities by the strengths of the metal−sulfur bonds. Similar investigations on the catalytic properties of bimetallic transition metal sulfide phases can give more insight in the mechanisms of hydrodesulfurization, e.g. in the interaction between MoS_2/WS_2 phases and promotor atoms. In this context, the cluster complexes such as [**1**][pts]−[**6**][pts] are used as starting materials for a systematic investigation on hydrotreating activities of bimetallic sulfide materials with molybdenum or tungsten as base metal component.[54] They also serve, as shown earlier,[17] on a molecular basis as model systems for the active centers of industrially used hydrotreating catalysts or for fundamental spectroscopic studies.

Acknowledgment. This work was supported by the European Commission (TMR Network "Metal Clusters in Catalysis and Organic Synthesis"; Contract FMRX-CT96-0091; postdoctoral grant to K.H.). P.Z. gratefully acknowledges the financial support of the MURST of Italy (Cofin. 2000). We also thank Ms. M. Christensen for the preparation of $[(H_2O)_9Mo_3S_4][pts]_4\cdot 9H_2O$ and $[(H_2O)_9W_3S_4][pts]_4\cdot 9H_2O$.

Supporting Information Available: An ORTEP plot for the cluster cation $[\mathbf{6}]^+$ and three X-ray crystallographic files, in CIF format. This material is available free of charge via the Internet at http//pubs.acs.org.

IC0205379

(48) Astruc, D. In *Electron transfer and radical processes in transition-metal chemistry*; Wiley-VCH: New York, 1996; Chapter 4.
(49) Pecorado, T. A.; Chianelli, R. R. *J. Catal.* **1981**, *67*, 430.
(50) Hermann, N.; Brorson, M.; Topsøe, H. *Catal. Lett.* **2000**, *65*, 169.
(51) Vissers, J. P. R.; Groot, C. K.; van Oers, E. M.; de Beer, V. H. J.; Prins, R. *Bull. Soc. Chim. Belg.* **1984**, *93*, 813.
(52) Nørskov, J. K.; Clausen, B. S.; Topsøe, H. *Catal. Lett.* **1992**, *13*, 1.
(53) Topsøe, H.; Clausen, B. S.; Topsøe, N.-Y.; Nørskov, J. K.; Ovesen, C. V.; Jacobsen, C. J. H. *Bull. Soc. Chim. Belg.* **1995**, *104*, 283.
(54) Herbst, K.; Brorson, M. Iridium Promoted Sulfided Mo/Al_2O_3 Catalysts for Hydrodesulfurization (HDS) and Hydrodenitrogenation (HDN). Presented at the 17th North American Catalysis Society Meeting, Toronto, Ontario, Canada, June 3−8, 2001; Technical Program, p 267.